MACRO-MECHANICAL AND MICROSCOPIC STUDY OF THE FATIGUE DAMAGE BEHAVIOUR OF A CARBON FABRIC/PPS THERMOPLASTIC COMPOSITE

IVES DE BAERE, LINSEY LAPEIRE, WIM VAN PAEPEGEM, SUBAREDDY DAGGUMATI, KIM VERBEKEN AND JORIS DEGRIECK.
Department of Materials Science and Engineering, Faculty of Engineering, Ghent University. Technologiepark-Zwijnaarde 903, B-9052 Zwijnaarde, Belgium.

ABSTRACT

This manuscript elaborates on the tension-tension fatigue behaviour of a carbon fabric reinforced polyphenylene sulphide. The damage behaviour will be investigated by (i) conducting fatigue experiments, in order to determine the macroscopic behaviour such as permanent deformation and stiffness degradation and (ii) a microscopic investigation using both optical and scanning electron (SEM) microscopy.
It may be concluded that for the $[(0°,90°)]_{4s}$ stacking sequence the material does not show significant stiffness reduction and that only limited permanent deformation is present. Furthermore, the material shows very brittle failure behaviour. For the $[(+45°,-45°)]_{4s}$ stacking sequence, however, a different behaviour manifests itself. Stiffness reduction does occur and there is a significant permanent deformation, in combination with a high rise in temperature, above the softening temperature of the matrix.

1. INTRODUCTION AND PRINCIPLE

Throughout the fatigue lifetime, damage can take many forms in fibre-reinforced composites (ref.1-2): (i) matrix cracks, (ii) fibre-matrix interface failure, (iii) fibre pull-out, (iv) delaminations, (v) fibre fracture. This damage affects the value of the elastic properties at an early stage. Especially in fatigue, the damage initiation phase can cause a pronounced drop of the elastic modulus of 5 to 10 %. In the next damage propagation phase, the stiffness continues to decrease gradually, ranging from a few percent for unidirectionally reinforced carbon composites to several tens of percents for multidirectional glass laminates (ref.3-5). Furthermore, most one-dimensional damage models for fibre-reinforced composites only account for the effect of damage on the stiffness (ref.6-8). As such, the main focus in the fatigue experiments described here is on the expected stiffness degradation and permanent deformation.

2. MATERIALS AND METHODS

2.1. Composite Material

The material used for the experiments was a 5-harness satin-weave carbon fabric-reinforced polyphenylene sulphide (PPS), of which there are three tons in the Airbus A380. The carbon PPS plates were hot pressed, two stacking sequences were used for this study, namely $[(0^o,90^o)]_{2s}$ and $[(+45^o,-45^o)]_{2s}$ where $(0^o,90^o)$ and (+45°,-45°) represent one layer of fabric. The in-plane elastic properties and the tensile strength properties are listed in Table 1. This material was supplied to us by Ten Cate Advanced Composites (The Netherlands).

Table 1 Elastic and strength properties of the CETEX® material.

E_{11} [GPa]	E_{22} [GPa]	ν_{12} [-]	G_{12} [GPa]	X_T [MPa]	ε_{11}^{ult} [-]	Y_T [MPa]	ε_{22}^{ult} [-]	S_T [MPa]
56.0	57.0	0.033	4.175	736	0.011	754.0	0.013	110.0

The test coupons were saw with a water-cooled diamond saw. The dimensions of the coupons are shown in Figure 1.

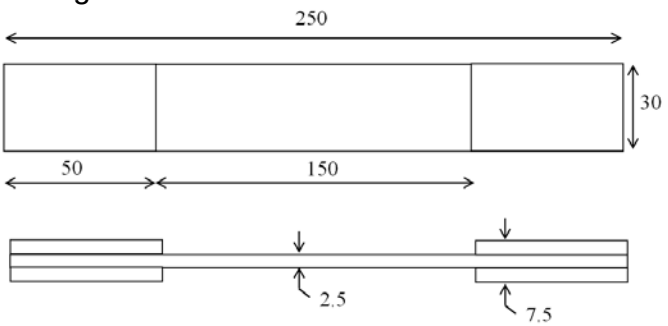

Figure 1 Dimensions of the used tensile coupon, equipped with straight-end tabs.

2.2. Equipment

All tensile tests were performed on a servo-hydraulic INSTRON 8801 tensile testing machine with a FastTrack 8800 digital controller and a load cell of ±100kN. For the registration of the tensile data, a combination of a National Instruments USB 6251 data acquisition card and the SCB-68 pin shielded connecter were used.
For the observation of the microscopic damage, a FEI XL30 Scanning Electron Microscope equipped with a LaB_6 filament was used on samples which were sputter-coated with an ultrathin Au layer.

3. EXPERIMENTS AND DISCUSSION

3.1. $[(0^o,90^o)]_{4s}$ Fatigue tests

Various experiments were performed, both at 2 Hz and 5 Hz loading frequency and for maximum stress levels varying between 550 MPa and 700 MPa, but all of them show similar behaviour, so only one of these experiments is illustrated here, namely a test between 0 and 650 MPa at 2 Hz. Figure 2 shows the evolution of the longitudinal strain and the temperature of this experiment. Since it is a load-controlled test, the amplitude of the strain corresponds with possible variations in stiffness and

as can be seen, no real stiffness degradation occurs. Moreover, there is no significant increase in permanent deformation, which can be seen from the evolution in the minimum value of the strain. When the run-in of a fatigue test is observed more closely, it can be seen that the limited permanent deformation tends to develop in the first fifty to sixty cycles. This explains why the minimum value of the permanent deformation does not start at zero in Figure 2.

It can also be noted that there is no significant change in temperature. The limited variations of the temperature are due the changes in the room temperature. The room where the experiments were conducted, has a climate control system but the variations in Figure 2 are within the range of this system. In general, for all of the uni-axial fatigue experiments, no significant variation in temperature occurred, and all changes can be ascribed to variations in room temperature.

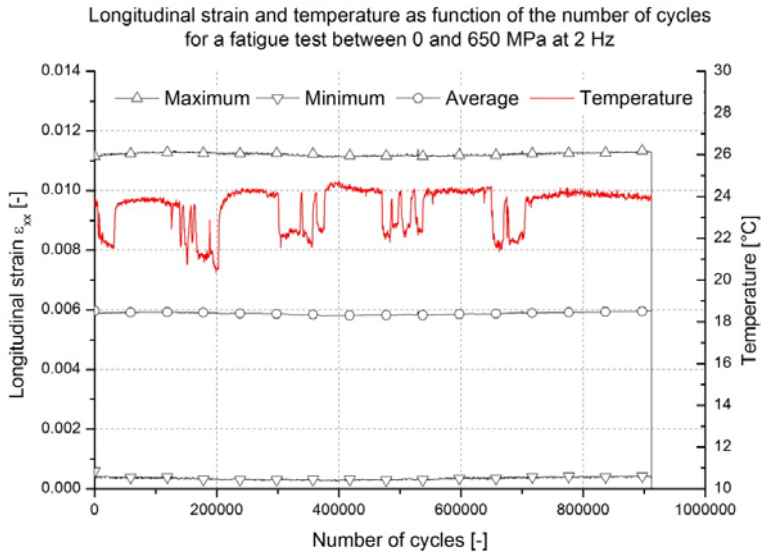

Figure 2 Maximum, minimum and mean value of the longitudinal strain and temperature as a function of the number of cycles for the 0-650 MPa tensile fatigue test at 2 Hz.

As previously mentioned, all conducted fatigue experiments show similar mechanical behaviour as the one illustrated above, so they are not commented on here. For more details and experimental results, the authors refer to (ref.10).

With respect to microscopic damage, Figure 3 shows a detailed SEM image of broken fibres of the fracture surface. Besides the fact that the carbon fibres show a brittle failure, it can clearly be noticed that in the fracture area, virtually no PPS is left on the fibres. The authors assume that the PPS is removed from the fibres due to friction of the fibre in the matrix.

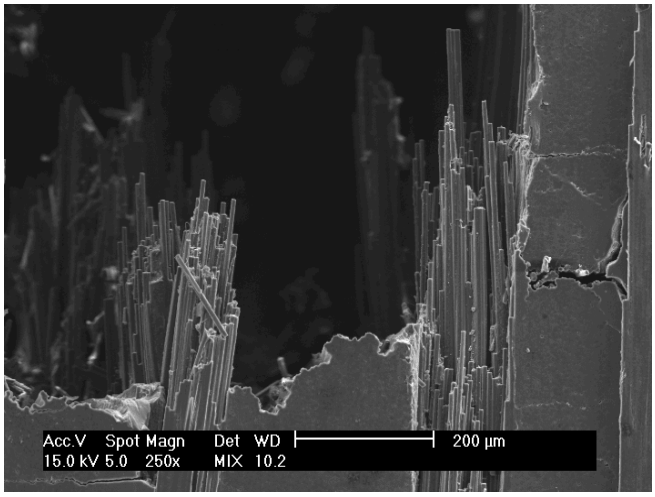

Figure 3 SEM of broken fibres on the fracture surface of the $[(0°,90°)]_{4s}$ specimen with a magnification of 250x.

Figure 4 illustrates the top surface of a $[(0°,90°)]_{4s}$ specimen with both SEM and optical microscopy; this crack pattern was visible over the entire specimen. For the SEM (Figure 4, left), typical 45° cracks were observed in the area where there is a crossing over of the warp and weft bundles. The cracks in the weft bundles can also clearly be seen (Figure 4, right).

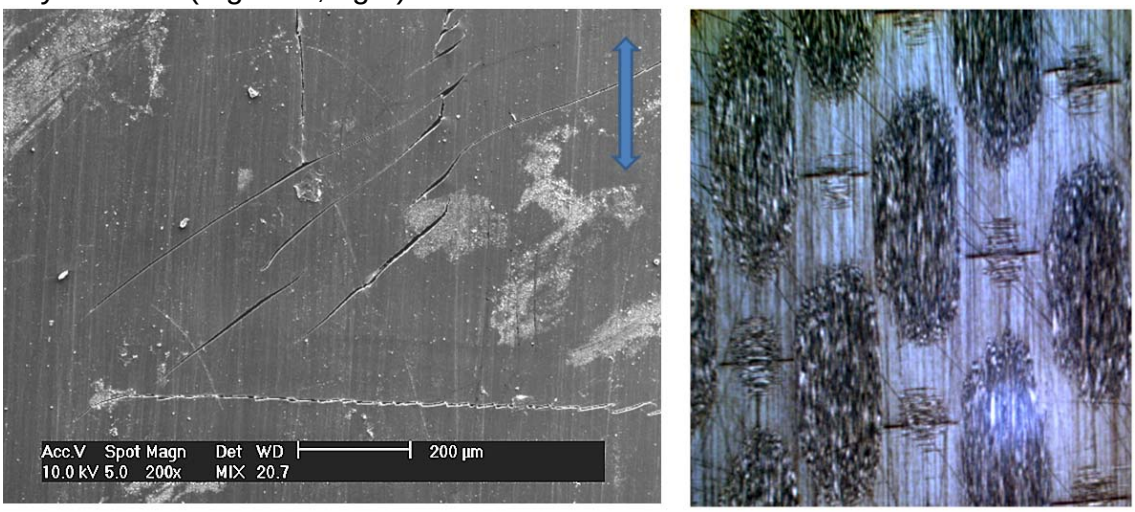

Figure 4 SEM of the top surface of the $[(0°,90°)]_{4s}$ specimen with a magnification of 200x (left) and optical microscopy with a magnification of 10x (right).

Finally, Figure 5 shows pictures of the polished side of the specimen both unloaded (a) and loaded till 650 MPa (b) taken after 680 000 cycles. It can clearly be seen that significant meta-delaminations exist. What could also be observed during the test was that the warp fibre bundles moved freely in the layers, meaning that these bundles are completely debonded from the PPS matrix.

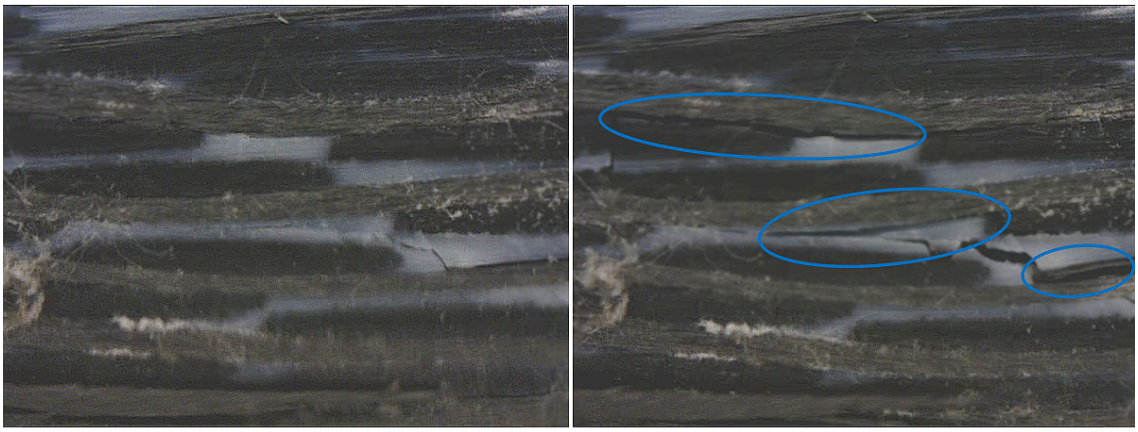

(a) unloaded (b) loaded

Figure 5 Illustration of the side of the specimen in both unloaded and loaded (650 MPa) state of a 650MPa@2Hz fatigue test, afters 680 000 cycles.

3.2. $[(+45^{o},-45^{o})]_{4s}$ Fatigue tests

Figure 6 illustrates the typical behaviour of the material under study when subjected to shear loads, for a test between 0 and 50 MPa at 2Hz loading frequency. In this picture, the evolution of the maximum, minimum and average value of the displacement during the fatigue experiment is plotted against the number of cycle for a test between τ_{min} = 0 MPa and τ_{max} = 50 MPa. As the test is done in load control with a constant stress ratio, the evolution of the displacement gives information on (i) the permanent deformation, by observing the evolution of the minimum value, where the specimen is unloaded and (ii) the shear stiffness, by observing the difference between the maximum and minimum level. The more the stiffness decreases, the bigger this difference becomes.

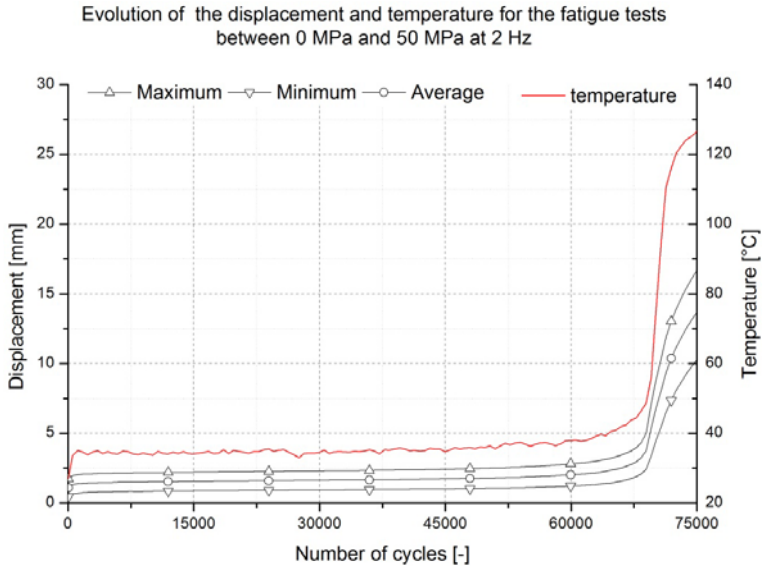

Figure 6 Maximum, minimum and mean value of the displacement and temperature as a function of the number of cycles till 'failure' for the 0-50 MPa tensile fatigue test at 2 Hz.

The behaviour of carbon PPS under shear load can be described in three stages. First, there is the run-in of the fatigue test, where a certain amount of permanent deformation occurs without an increase in temperature. This happens in the first

dozen cycles and is therefore not visible in Figure 6, but this is the reason why the minimum displacement does not start at zero in this picture. Then, there is a steady-state phase, where there is a gradual increase in permanent deformation, without any significant increase in temperature, but where damage initiates and grows and finally, there is a the end-of-life phase, where there is a sudden increase in temperature, above the softening temperature of the matrix (90°C) and a sudden growth in permanent deformation. This causes severe deformation, which the authors consider 'failure' of the specimen. However, the specimen does not break during this 'end-of life' phase, it tends to deform into a 'dumbbell' like shape, which is illustrated in Figure 7, where the specimen N2, on which a 0-50 MPa, 2 Hz fatigue experiment was done, can be compared with another specimen which is still to be tested, but with the same dimensions as specimen N2 had before testing.

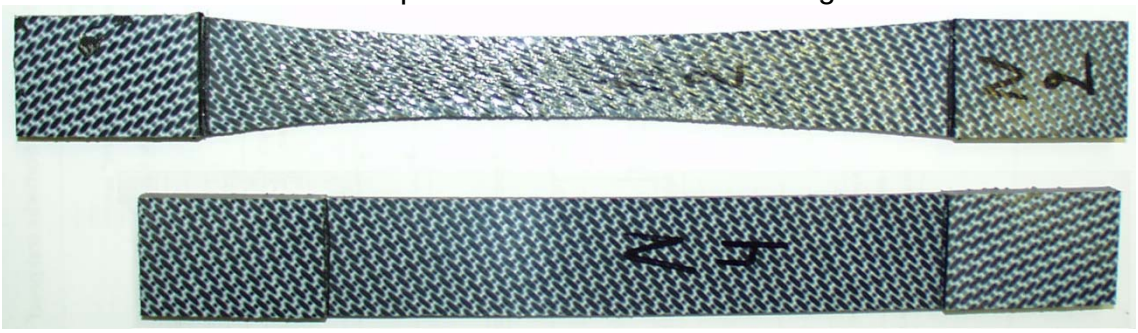

Figure 7 Deformed (top) and undeformed (bottom) $[(+45°,-45°)]_{4s}$ specimen.

To determine the damage in the specimen, scanning electron microscopy was used on a similar sample, on which the test was stopped when the 'end-of-life' phase was reached. A sample was cut out of the necked area and both the top and the side surface where investigated. Figure 8 illustrates the side of the specimen and as clearly visible, a lot of damage is present. Not only a significant amount of splitting of the fibre bundles occurs, but almost every layer has delaminated. When observing the close-up (Figure 8, right), it can be noticed that there is almost no PPS attached to the fibres, similar to the fracture area of the $[(0°,90°)]_{4s}$ specimens.

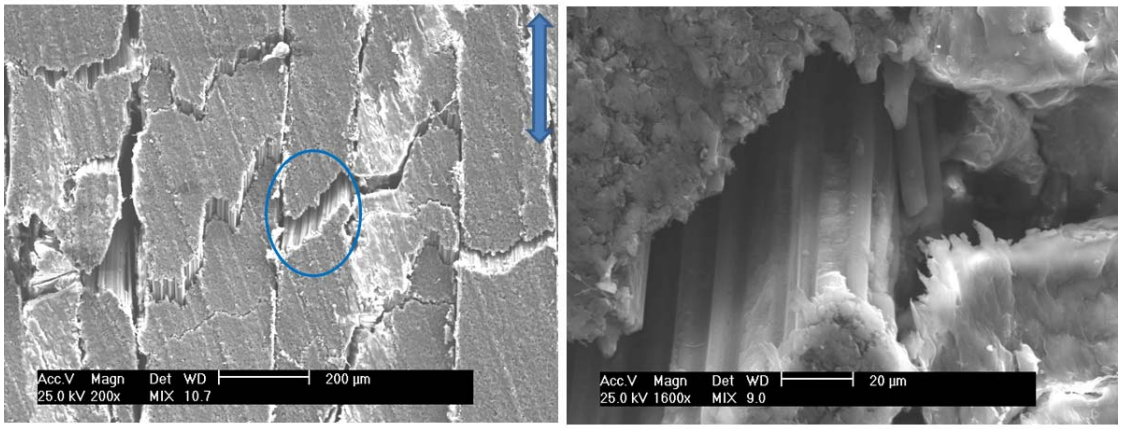

Figure 8 SEM on the side of the $[(+45°,-45°)]_{4s}$ specimen with a magnification of 200x left and 1600x right.

Figure 9 illustrates the top side of the specimen and this type of damage occurs over the entire specimen. Again, the splitting of the fibre bundles can clearly be seen, but also, triangular gaps can be found where the bundles cross over each other and a stress concentration is present. Similar cracks were found for the $[(0°,90°)]_{4s}$ tests (see Figure 4).

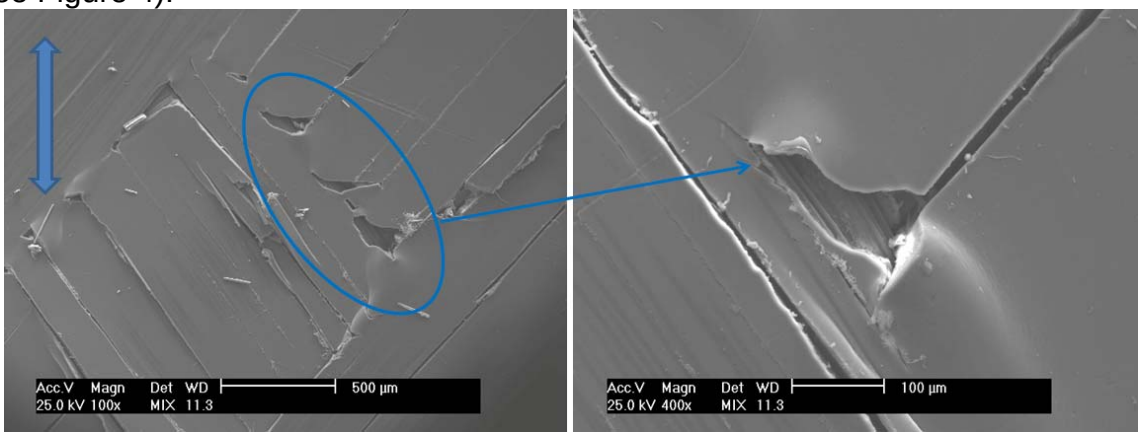

Figure 9 SEM on the topside of the $[(+45°,-45°)]_{4s}$ specimen with a magnification of 100x left and 400x right, illustrating the stress concentration at the bundle cross-over.

As such, the typical behaviour from Figure 6 can be explained as follows. Due to the shear loads, there is a gradual increase in damage, mainly in the fibre-matrix interface, causing the fibres to debond from the matrix and the load is transmitted due to friction of the matrix on the fibre. This friction causes a local elevation in temperature, resulting in local softening of the matrix and thus in more fibre debonding. This initially results in a steady state phase, because of the cooling effect of the surrounding air. At a certain point, when a critical amount of damage is present, this process becomes unstable, resulting in a significant increase in temperature of the entire specimen, above the softening temperature of the matrix, causing the change of shape into a dumbbell.

4. CONCLUSIONS

This paper investigated the tension-tension fatigue behaviour of a carbon fabric reinforced polyphenylene sulphide. The mechanical behaviour of the $[(0°,90°)]_{4s}$ stacking sequence, meaning when the material is loaded along the fibre direction, is characterised as follows: only very little permanent deformation occurs during the fatigue lifetime, and most of it develops during the first hundred cycles. Also, there is no stiffness degradation present and failure is quite brittle and occurs very sudden, without any detectable warning.

The mechanical behaviour of the $[(+45°,-45°)]_{4s}$ stacking sequence, meaning when the material is subjected to in-plane shear loads shows a very different behaviour and it can be described in three stages: (i) run-in of the fatigue test, where a certain amount of permanent deformation occurs without an increase in temperature; (ii) a steady-state phase, where there is a gradual increase in permanent deformation, without an increase in temperature and (iii) the end-of-life phase, where there is a

sudden increase in temperature, above the softening temperature of the matrix and a sudden growth in permanent deformation.
When observing the occurring damage in both cases, it can be remarked that there is a significant amount of damage. Fibre bundle splitting occurs, as well as local cracks due to the stress concentrations near the fibre cross-overs. With respect to the $[(0°,90°)]_{4s}$ stacking sequence, a lot of meta-delaminations are present and some warp bundles are no longer bonded to the matrix. Nevertheless, despite the fact that there is a lot of damage inside the material, it is still capable of carrying significant loads, both along the fibres and under in-plane shear.

ACKNOWLEDGEMENTS

The authors are highly indebted to the Fund of Scientific Research – Flanders (F.W.O.) for sponsoring this research and to Ten Cate Advanced Composites for supplying the material.

REFERENCES

[1] Herakovich, C.T.. Mechanics of fibrous composites. John Wiley & Sons, Inc, New York, 1998.

[2] Talreja, R. Damage and fatigue in composites - A personal account. Composite Science and Technology 68 (13) (2008) pp: 2585-2591

[3] Shirazi, A and Varvani-Farahani, A. A Stiffness Degradation Based Fatigue Damage Model for FRP Composites of (0/theta) Laminate Systems. Applied Composite Materials 17 (2), (2010) pp: 137-150

[4] Giancane, S., Panella, F. W. and Dattoma, V. Characterization of fatigue damage in long fiber epoxy composite laminates. International Journal of Fatigue 32 (1), (2010) pages: 46-53

[5] Taheri-Behrooz F., Shokrieh, M M. and Lessard, LB. Residual stiffness in cross-ply laminates subjected to cyclic loading. Composite Structures 85 (3), (2008) pp: 205-212

[6] Hwang, W. and Han, K.S. Fatigue of composites - Fatigue modulus concept and life prediction. Journal of Composite Materials, 20, (1986), pp 154-165.

[7] Whitworth, H.A.. Modelling stiffness reduction of graphite epoxy composite laminates. Journal of Composite Materials, 21(1987), pp 362-372.

[8] Yang, J.N., Jones, D.L., Yang, S.H. and Meskini, A.. A stiffness degradation model for graphite/epoxy laminates. Journal of Composite Materials, 24 (1990), pp 753-769.

[9] De Baere I., Van Paepegem W. and Degrieck J., Comparison of the modified three-rail shear test and the $[(+45°,-45°)]_{ns}$ tensile test for pure shear fatigue loading of carbon fabric thermoplastics. Fatigue and Fracture of Engineering Materials & Structures. Vol. 31 (6) (2008) pp: 414-427

[10] De Baere I, Experimental and Numerical Study of Different Setups for Conducting and Monitoring Fatigue Experiments of Fibre-Reinforced Thermoplastics, Ph.D. thesis. Gent, Belgium, Ghent University, 2008. ISBN 978-90-8578-196-7